

A WFE and hybrid FE/WFE technique for the forced response of stiffened cylinders

Fabrizio Errico*¹, M. Ichchou¹, S. De Rosa², O. Bareille¹ and F. Franco²

¹LTDS, Laboratoire de Tribologie et Dynamique des Systems, Ecole Centrale de Lyon, 36 Avenue Guy de Collongue, 69134 Écully, France

²Pasta-Lab, Laboratory for promoting experiences in aeronautical structures and acoustics, Dipartimento di Ingegneria Industriale Sezione Aerospaziale, Università degli Studi di Napoli "Federico II", Via Claudio 21, 80125 Napoli, Italy

(Received July 24, 2017, Revised July 30, 2017, Accepted July 31, 2017)

Abstract. The present work shows many aspects concerning the use of a numerical wave-based methodology for the computation of the structural response of periodic structures, focusing on cylinders. Taking into account the periodicity of the system, the Bloch-Floquet theorem can be applied leading to an eigenvalue problem, whose solutions are the waves propagation constants and wavemodes of the periodic structure. Two different approaches are presented, instead, for computing the forced response of stiffened structures. The first one, dealing with a Wave Finite Element (WFE) methodology, proved to drastically reduce the problem size in terms of degrees of freedom, with respect to more mature techniques such as the classic FEM. The other approach presented enables the use of the previous technique even when the whole structure can not be considered as periodic. This is the case when two waveguides are connected through one or more joints and/or different waveguides are connected each other. Any approach presented can deal with deterministic excitations and responses in any point. The results show a good agreement with FEM full models. The drastic reduction of DoF (degrees of freedom) is evident, even more when the number of repetitive substructures is high and the substructures itself is modelled in order to get the lowest number of DoF at the boundaries.

Keywords: wave finite element; cylinders dynamics; wave propagation; periodic structures; forced response

1. Introduction

The finite element method (FEM) is widely considered as one of the most used and appealing methods for solving problems concerning the dynamics of complex structures. Typically used for modal and dynamic applications, this method enhances the operator to obtain information about the vibrational levels from the discretized model of the whole structure. However, in many engineering applications, high frequency vibrations become significant. In these cases, the proper discretization

*Corresponding author, E-mail: fabrizio.errico@ec-lyon.fr

would require a huge number of elements even for simple and relatively small structural systems, leading to cumbersome computational cost.

Moreover, the development of new models is complicated because of the wide frequency range of interest. In the Low Frequency range the response exhibits isolated modal resonances and it has local characteristics, as spatial response peculiarities or constraint effects on the global response. In this case the deterministic techniques are still the preferred ones. At high frequencies the response is diffuse and does not present specific resonances. The averaged response is a good representation of the system dynamics. Energy based methods are used therefore. On the other hand, the mid frequencies are a transition zone, for which well-established prediction techniques are not yet available.

Noticing many engineering structures as being periodic, even if not being designed to take full advantage of the features of the periodicity itself, the Wave Finite Element Method, candidates itself to be a feasible approach to partially overcome the previous issues, making use of the Periodic Structure Theory Brillouin (1953) to re-built a spatially distributed response with the analysis of the dynamics of a single repetitive element.

Periodic structures, in fact, are supposed to be constituted by a set of identical elementary cells, repeated along one, two or three directions. Once the cell structural features are obtained through FE techniques, the entire WFE method is based on the analysis of the wave propagation in the media and algebraic matrix operations on reduced-size models.

Perhaps one of the first application of the method was the work Mead Mead (1996). Many authors, then, reformulated the methodology to take into account different factors. This helped to assess and frame basically the technique itself.

The research in this peculiar field is very intense nowadays. The potentiality of the WFE is tangible and it may enhance the modern industry to overcome actual barriers of computational cost. A deeper understanding of wave propagation will provide the background necessary for further innovations in this field.

2. The wave finite element method

A wave can be described as a disturbance that travels through a medium, transporting energy from its source location to others, without matter flux. A medium is intended as a material that carries the wave, and it should be considered as a collection of particles capable to interact with each other D'Alessandro (2014).

2.1 The bloch-floquet theorem

Bloch's theorem represents a generalisation, in solid-state physics, of the Floquet's theorem for 1-dimensional problem. The theorems says that in an infinite periodic media, the field, whatever it is (displacement, velocity, force, etc), in one point is connected to the same field in another point, whose distance from the previous one is r , by a magnitude variation and a phase shift. The wavefunction in the periodic media are assumed as being Bloch waves, in the form of Eq. (1). A plane free wave that propagates along a structure is assumed to take the form of a Bloch wave ψ_r

$$\{\psi_r\} = e^{-i\beta r} \{u_r\} \quad (1)$$

Where r is the distance vector, β is the propagation constant, u_r is a spatially periodic function.

Bloch showed how electron wave functions in a crystals have a basis consisting entirely of Bloch wave energy eigenstates. This reflect in periodic structures to exhibit pass-bands and stop-bands, in that each disturbance can propagate freely only in specific frequency ranges, otherwise they decay with distance Manconi *et al.* (2008).

2.2 2D Periodicity conditions

Lets, now, consider a rectangular panel (Fig. 1) where L_x , L_y are the in-plane dimensions and h is the thickness. A periodic segment of the panel with dimensions dx and dy is modelled using FE. No displacement field is supposed, as in SFEM, and the cell matrix can be obtained through extraction from common FE commercial software. The entries for each Degree of Freedom (DoF), for every node laying on the same edge of the segment, say edges 1, 2, 3 and 4 as in Fig. 1, are placed in the mass and stiffness matrices so that the vector of displacements can be written as [9]: $\{q\} = \{q_1 \ q_2 \ q_3 \ q_4\}$.

The time-harmonic equation of motion of the segment assuming uniform and structural damping for all the DoF can be written as

$$[K(1 - \eta i) - \omega^2 M]\{q\} = \{F\} \tag{2}$$

Where η is the structural damping coefficient, ω is the angular frequency and F the vector of the nodal forces [9]. It is important to remind that damping can be introduced also with a specific matrix, not merely as structural one. Different damping model can be used, but then, the dynamic stiffness matrix, can always be written as

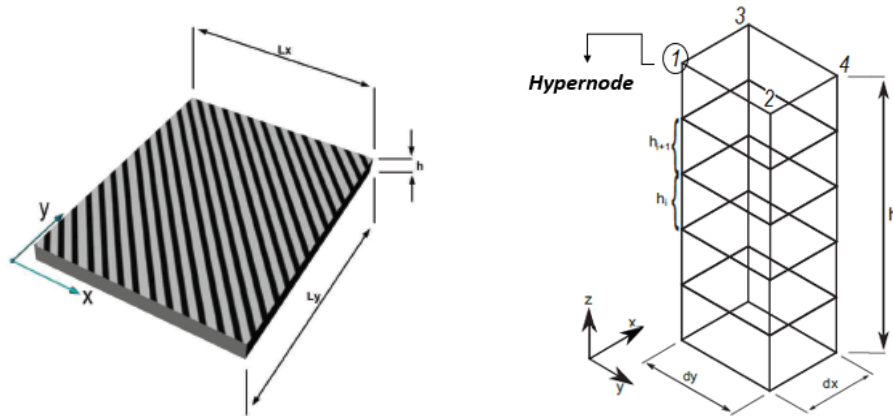


Fig. 1 Rectangular Panel and its modelled periodic cell [7]

$$\begin{bmatrix} D_{11} & D_{12} & D_{13} & D_{14} \\ D_{21} & D_{22} & D_{23} & D_{24} \\ D_{31} & D_{32} & D_{33} & D_{34} \\ D_{41} & D_{42} & D_{43} & D_{44} \end{bmatrix} \begin{Bmatrix} q_1 \\ q_2 \\ q_3 \\ q_4 \end{Bmatrix} = \begin{Bmatrix} F_1 \\ F_2 \\ F_3 \\ F_4 \end{Bmatrix}$$

So using the Floquet theory, or Bloch's theorem, for a rectangular segment and assuming a time-harmonic response, the displacements and forces of each edge can be written, as before, as a function of a single edge/corner displacement and forces Chronopoulos *et al.* (2013). Taking the hypernode (union of all the nodes in the thickness on the same segment) 1 (see Fig. 1) as the edge of reference we have

$$\{q_2\} = \lambda_X \{q_1\} \quad \{q_3\} = \lambda_Y \{q_1\} \quad \{q_4\} = \lambda_X \lambda_Y \{q_1\} \quad (3)$$

$$\{F_2\} = \lambda_X \{F_1\} \quad \{F_3\} = \lambda_Y \{F_1\} \quad \{F_4\} = \lambda_X \lambda_Y \{F_1\} \quad (4)$$

$$\begin{Bmatrix} q_1 \\ q_2 \\ q_3 \\ q_4 \end{Bmatrix} = \begin{Bmatrix} \mathbf{I} \\ \lambda_X \mathbf{I} \\ \lambda_Y \mathbf{I} \\ \lambda_X \lambda_Y \mathbf{I} \end{Bmatrix} \{q_1\}$$

Since equilibrium requires that the sum of the nodal forces at each node is zero, we have

$$\left\{ \mathbf{I} \quad \lambda_X^{-1} \mathbf{I} \quad \lambda_Y^{-1} \mathbf{I} \quad \lambda_X^{-1} \lambda_Y^{-1} \mathbf{I} \right\} \begin{Bmatrix} F_1 \\ F_2 \\ F_3 \\ F_4 \end{Bmatrix} = \mathbf{0}$$

With $\lambda_j = e^{-i\mu_j \Delta_j}$, where μ is the propagation constant and Δ_j the distance in "j" direction between reference and target cell.

As for classic FEM, the dynamic stiffness matrix of Eq. (2) is a NxN matrix, where N is the number of the total DOF of the cell. Substituting periodicity conditions in Eq. (2), we obtain a reduced matrix of size n , where $n < N$, equal to the reference side, in this case the hypernode "1".

$$\left\{ \mathbf{I} \quad \lambda_X^{-1} \mathbf{I} \quad \lambda_Y^{-1} \mathbf{I} \quad \lambda_X^{-1} \lambda_Y^{-1} \mathbf{I} \right\} \mathbf{D} \begin{Bmatrix} \mathbf{I} \\ \lambda_X \mathbf{I} \\ \lambda_Y \mathbf{I} \\ \lambda_X \lambda_Y \mathbf{I} \end{Bmatrix} \{q_1\} = \mathbf{0}$$

$$[\mathbf{K}_r - \omega^2 \mathbf{M}_r] \{q\} = \mathbf{D}_r \{q\} = \mathbf{0} \quad (5)$$

2.3 The eigenvalue problem

Using Eq. (5) and exploiting all the terms, it is possible to write the problem in this form

$$\begin{aligned}
& [(\mathbf{D}_{11} + \mathbf{D}_{22} + \mathbf{D}_{33} + \mathbf{D}_{44})\lambda_X \lambda_Y + \\
& \quad (\mathbf{D}_{12} + \mathbf{D}_{34})\lambda_X^2 \lambda_Y + \\
& (\mathbf{D}_{13} + \mathbf{D}_{24})\lambda_X \lambda_Y^2 + \mathbf{D}_{32}\lambda_X^2 + \mathbf{D}_{23}\lambda_Y^2 + \\
& \quad (\mathbf{D}_{21} + \mathbf{D}_{43})\lambda_Y + (\mathbf{D}_{31} + \mathbf{D}_{42})\lambda_X + \\
& \quad \mathbf{D}_{14}\lambda_X^2 \lambda_Y^2 + \mathbf{D}_{41}] \{q\} = \mathbf{0}
\end{aligned} \tag{6}$$

Considering the transpose of Eq. (6) divided by $\lambda_Y \lambda_X$, it can be proved that the solutions come in pairs involving (λ_Y, λ_X) and $(\lambda_Y^{-1}, \lambda_X^{-1})$ for a given real frequency ω . These of course represent the same disturbance propagating in the four directions $\pm\theta, \pi \pm\theta$, with respect to a common reference system Manconi *et al.* (2008).

Equation 6 gives eigenproblems relating λ_Y, λ_X and ω , whose solutions give FE estimates of the wave modes and dispersion relations for the continuous structure. Three different algebraic eigenvalue problems are possible since the problem is three parametric. If (μ_x) and (μ_x) are assigned and real, a linear eigenvalue problem results in ω for propagating waves. If the frequency ω and wavenumber are given, the other one is extracted. This is the case of an incident wave on a boundary, whose trace wavenumber is known. In this case the problem becomes a quadratic eigenproblem with twice the solutions.

When the frequency and θ are prescribed the problem might become a transcendental eigenvalue problem. Deeper details are available in Manconi *et al.* (2008).

2.4 1D Periodicity conditions

The description of waves travelling in a periodic structure is achieved by considering the eigenproblem which derives from imposing the Floquet's conditions to a cell or a substructure, whose stiffness and mass matrices can be gathered from classic FE models. In the 1D case the periodicity conditions are defined by imposing the equilibrium of the displacement and forces among the common hypernode of two subsequent cells.

Starting from the DSM (Dynamic Stiffness Matrix) problem of a partial assemble of cells, reordering the DoFs so that internal, left and right nodes's degrees of freedom are properly separated in the following way, we can move to the transfer matrix. In the following equations the left and right side hypernodes are defined with the letters L and R respectively.

$$\begin{bmatrix} \mathbf{D}_{ll} & \mathbf{D}_{lr} & \mathbf{D}_{li} \\ \mathbf{D}_{rl} & \mathbf{D}_{rr} & \mathbf{D}_{ri} \\ \mathbf{D}_{il} & \mathbf{D}_{ir} & \mathbf{D}_{ii} \end{bmatrix} \begin{Bmatrix} q_L \\ q_R \\ q_I \end{Bmatrix} = \begin{Bmatrix} F_L \\ F_R \\ 0 \end{Bmatrix}$$

Eliminating internal degrees of freedom (I) we get our base-work equation, as previously described.

$$\begin{bmatrix} \mathbf{D}_{LL} & \mathbf{D}_{LR} \\ \mathbf{D}_{RL} & \mathbf{D}_{RR} \end{bmatrix} \begin{Bmatrix} \mathbf{q}_L \\ \mathbf{q}_R \end{Bmatrix} = \begin{Bmatrix} \mathbf{F}_L \\ \mathbf{F}_R \end{Bmatrix}$$

With

$$\mathbf{D}_{BB} = \mathbf{D}_{BB} - \mathbf{D}_{Bi} \mathbf{D}_{ii}^{-1} \mathbf{D}_{iB} \quad (7)$$

Where B stands for cell boundary, left or right.

Imposing continuity of displacements and equilibrium of forces at the interface between adjacent cell S and $(S+1)$, and putting all in a matrix form we can get the Transfer Matrix, \mathbf{T} . It relates the nodal displacements and forces (evaluated on the left side) between two adjacent substructures.

$$[\mathbf{T}] = \begin{bmatrix} -\mathbf{D}_{LR}^{-1} \mathbf{D}_{LL} & \mathbf{D}_{LR}^{-1} \\ -\mathbf{D}_{RL} + \mathbf{D}_{RR} \mathbf{D}_{LR}^{-1} \mathbf{D}_{LL} & -\mathbf{D}_{RR} \mathbf{D}_{LR}^{-1} \end{bmatrix}$$

It has been shown Mencik (2010) that the eigenvalues of the transfer matrix occur in reciprocal pairs as , $\lambda_j^+ = 1/ \lambda_j^-$ corresponding to pairs of positive (+) and negative (-) going waves, respectively. Associated with these eigenvalues are the positive and negative going eigenvectors ϕ_j^- and ϕ_j^+ respectively, which will also be referred to as wavemodes Mencik (2010). These are the displacement and force distributions in the substructure section. Every wavemode can be partitioned into a sub-vector of DoFs and internal forces/moments as in Eq. (8).

Positive waves are characterized by $|\lambda_j^+| < 1$, which means that if the wave propagates its amplitude must decrease in travelling. If $|\lambda_j^+| = 1$ then the time average power transmission in the positive direction is evaluated to select the positive and negative going waves. With that, one can group the wavemodes as

$$\Phi_q^+ = \begin{bmatrix} [\phi_{1,q}^+] & [\phi_{n,q}^+] \end{bmatrix} \quad \Psi_q^+ = \begin{bmatrix} [\psi_{1,q}^+]^T & [\psi_{n,q}^+]^T \end{bmatrix} \quad (8)$$

A transformation between the physical domain, where the system's behaviour is described in terms of q and f , and the wave domain, where the behaviour is described in terms of waves of amplitudes a^+ and a^- travelling in the positive and negative directions is derived through these matrices Renno et al. (2014). In particular

$$\begin{Bmatrix} \mathbf{q}_L \\ \mathbf{f}_L \end{Bmatrix} = \begin{bmatrix} \Phi_q^+ & \Phi_q^- \\ \Phi_f^+ & \Phi_f^- \end{bmatrix} \begin{Bmatrix} \mathbf{a}^+ \\ \mathbf{a}^- \end{Bmatrix}$$

Where $\mathbf{a}^{+,-}$ are the wave amplitudes of the positive and negative going waves.

2.5 The model reduction

The proper selection of propagating waves can be done considering the imaginary part of the propagating constant of each wavemode. The criteria used are to be chosen case by case and a well established method is still not available in literature. In the present work the criteria used can be summarized in the following way, considering j as a tolerance parameter

$$\text{imag}|k_i dX| < j \quad (9)$$

Where k_i and dX are the wavenumber associated to the wavemode i and the spatial step among the cells of the periodic structure. Physically this means considering the only contribution, to structural response, of the propagating or close-to propagating waves. At each frequency step, when and if new wavemodes cut-on, these are included in the wave base.

However, a remark has to be made about this. The evanescent field might still have a significant effect on the response around the excitation point. On the other hand, as said, the effect is negligible as soon as we analyse the field far from the singularity. The ideal criteria would select correctly the number of waves to retain in the wave base considering also the distance from the excitation point.

3. Forced vibrations

3.1 The direct field

Lets write the continuity of displacements and the equilibrium of the force at the excitation point using the wave-base expansion, from which we can rewrite the equilibrium equations in matrix form.

$$\begin{bmatrix} \Phi s_q^+ & -\Phi s_q^- \\ \Phi s_f^+ & -\Phi s_f^- \end{bmatrix} \begin{Bmatrix} e^+ \\ e^- \end{Bmatrix} = \begin{Bmatrix} \mathbf{0} \\ \mathbf{f}_{ext} \end{Bmatrix}$$

Where $e^{+,-}$ is the vector of the amplitudes of the wavemodes. They define, in other words, the directly excited field. The inversion of the above left-hand side matrix can lead to numerical errors, especially for complex structures and cell shapes. A solution to avoid this is exploiting the orthogonality of the left and right eigenvectors, pre-multiplying both sides of the previous equation by the matrix of left eigenvectors properly rearranged to get to the following form D'Alessandro (2014), Waki *et al.* (2009).

$$\begin{Bmatrix} e^+ \\ e^- \end{Bmatrix} = \begin{Bmatrix} \Psi s_f^+ \mathbf{f}_{ext} \\ -\Psi s_f^- \mathbf{f}_{ext} \end{Bmatrix}$$

This, of course, requires a left-eigenvalue problem, whose eigenvectors are $\Psi s_f^{+,-}$, to be solved too. It is worth underline how the use of the force wavemodes is different from the use of the displacement ones, shown in [Waki *et al.* (2009)], and it has proved to lead to accurate results.

The wave amplitudes $e^{-,+}$ are the amplitudes of the directly excited waves. These move in both the sides of the now uni-dimensionalised problem. Fig. 2 can be used as illustrative reference.

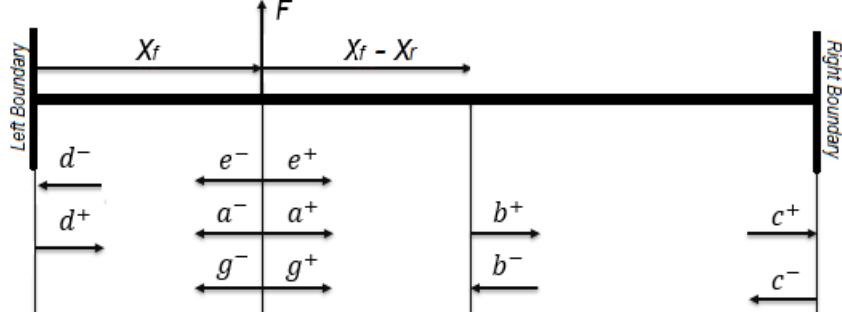


Fig. 2 Waves in a finite structure excited by point load

3.2 Waves at boundaries

Waves incident upon discontinuities and boundaries are partially reflected, transmitted and absorbed. Instead, in the case of elastic boundary conditions, an incident wave is only reflected, without any transmission.

Considering a generic wave of amplitude \mathbf{h}^+ travelling in the medium, we can model the reflection and the subsequent opposite-going wave amplitude, \mathbf{h}^- , with the use of reflection matrices at boundaries.

Considering also \mathbf{R} as the matrix of reflection coefficients, which depends on the type of constraint, the wave problem at the boundaries can be expressed as $\mathbf{h}^{+, -} = \mathbf{R}\mathbf{h}^{-, +}$. Each boundary condition can always be expressed in the form: $\mathbf{A}\mathbf{f} + \mathbf{B}\mathbf{q} = \mathbf{0}$.

Substituting the wave base expansion for forces and displacements

$$\begin{aligned} \mathbf{R}_{right} &= -(\mathbf{A}\Phi s_f^- + \mathbf{B}\Phi s_q^-)^{-1}(\mathbf{A}\Phi s_f^+ + \mathbf{B}\Phi s_q^+) \\ \mathbf{R}_{left} &= -(\mathbf{A}\Phi s_f^+ + \mathbf{B}\Phi s_q^+)^{-1}(\mathbf{A}\Phi s_f^- + \mathbf{B}\Phi s_q^-) \end{aligned} \quad (10)$$

Where the matrices \mathbf{A} and \mathbf{B} are dependent on the type of constrain, as said. In the case of force-free boundaries, for example, $\mathbf{A} = \mathbf{I}$ and $\mathbf{B} = \mathbf{0}$.

3.3 Waves propagation

Moving in the medium, the amplitude of all the waves changes, depending on the distance and the wave characteristics itself.

Their variations can be derived by applying the definition of propagation constant. For instance, if the waveguide has n wave components, the waves amplitudes at two points a distance x apart are given by: $\mathbf{h}^+ = \mathbf{Tr} \mathbf{s}^+$, where \mathbf{Tr} is the wave propagation matrix. It can be expressed as

$$\mathbf{Tr}(x) = \text{diag}\left(e^{-ik_1x}, e^{-ik_2x}, \dots, e^{-ik_nx}\right) \quad (11)$$

All the elements of the wave propagation matrix have a magnitude less or equal to the unity, by definition.

3.4 Incident field and waves superposition

Once the amplitudes of directly excited wave are known, we can calculate the waves amplitudes at a given response point by considering the excitation, reflection and propagation relations.

Using again Fig. 2 as reference we can evaluate the amplitude of waves in the reference point.

The following is the set of equilibrium equation. The whole set is made of algebraic equations in matrix form and thus the ease of use is impressive.

At the excitation location, one can sum the incident and direct field

$$\begin{aligned} a^+ &= e^+ + g^+ \\ g^- &= e^- + a^- \end{aligned} \quad (12)$$

At boundaries the following reflection relations are valid

$$\begin{aligned} c^- &= \mathbf{R}_{right}c^+ \\ d^+ &= \mathbf{R}_{left}d^- \end{aligned} \quad (13)$$

At the same time along the waveguide, the following propagation relations hold

$$\begin{aligned} g^+ &= \mathbf{Tr}(x_f)d^+ \\ d^- &= \mathbf{Tr}(x_f)g^- \\ a^- &= \mathbf{Tr}(L - x_f)c^- \\ c^+ &= \mathbf{Tr}(x_f)a^+ \end{aligned} \quad (14)$$

Using the reflection relations at the boundaries and considering the propagating matrices, then, the wave amplitudes at excitation point are

$$a^+ = [\mathbf{I} - \mathbf{Tr}(x_f)\mathbf{R}_{left}\mathbf{Tr}(L)\mathbf{R}_{right}\mathbf{Tr}(L - x_f)]^{-1} [e^+ + \mathbf{Tr}(x_f)\mathbf{R}_{left}\mathbf{Tr}(x_f)e^-] \quad (15)$$

$$a^- = [\mathbf{I} - \mathbf{Tr}(L - x_f)\mathbf{R}_{right}\mathbf{Tr}(L)\mathbf{R}_{left}\mathbf{Tr}(x_f)]^{-1} [e^- + \mathbf{Tr}(L - x_f)\mathbf{R}_{right}\mathbf{Tr}(L - x_f)e^+] - e^- \quad (16)$$

The adopted approach allows numerical stability. In fact, the above solutions are well-conditioned because the matrices being inverted are diagonally dominant and the element of the wave propagation matrices are less than or equal to the unity D'Alessandro (2014).

The response in the reception point can be then calculated applying the propagation relations. For example, if the response point is over the excitation one

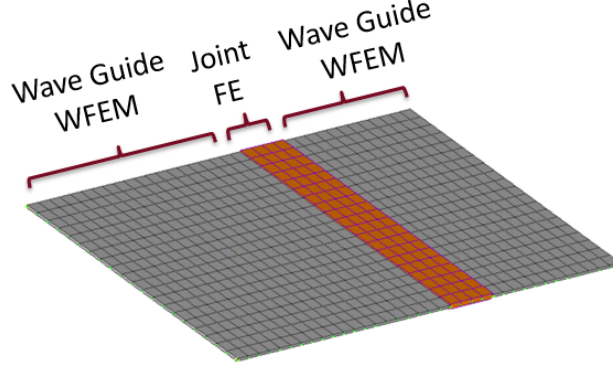


Fig. 3 Simple representation of two in-plane jointed waveguides

$$\begin{aligned}
 b^+ &= \mathbf{Tr}(x_{resp} - x_f)a^+ \\
 b^- &= \mathbf{Tr}(L - x_{resp})\mathbf{R}_{right}\mathbf{Tr}(L - x_{resp})b^+
 \end{aligned}
 \tag{17}$$

4. The hybrid FE/WFE method

In general the structures might not be fully periodic. It might happen, however, that the entire structure can be identified as the sum of periodic parts connected through joints. In this cases the technique presented above can still be considered valid if the scattering around the joint is taken into account.

4.1 The scattering matrix

When discontinuities such as linear or complex joints and boundaries, the scattering properties become largely impactful on the structural behaviour. Considering a junction as in Fig. 3 one can analyse the scattering properties taking into account the waves in the first and second waveguide, in terms of incident and outgoing (reflected and transmitted) wave amplitudes along the junction itself. These are showed in Fig. 4.

The scattering matrix \mathbf{s} can be defined taking into account what just said and thus has the following expression

$$\begin{Bmatrix} \mathbf{a}_1^- \\ \mathbf{a}_2^- \end{Bmatrix} = \mathbf{s} \begin{Bmatrix} \mathbf{a}_1^+ \\ \mathbf{a}_2^+ \end{Bmatrix}$$

with

$$\mathbf{s} = \begin{bmatrix} \mathbf{r}_{11} & \mathbf{t}_{12} \\ \mathbf{t}_{21} & \mathbf{r}_{22} \end{bmatrix}$$

Where \mathbf{r}_{ii} are the reflection matrices and \mathbf{t}_{ji} are the transmission matrices among the discontinuity.

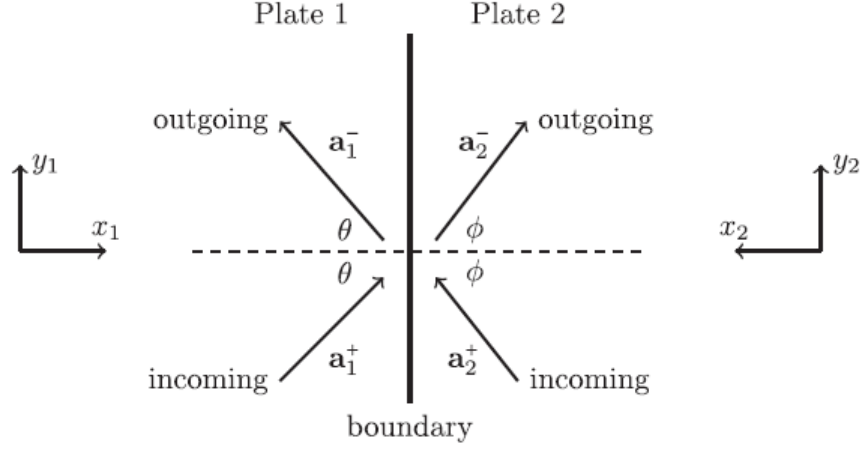


Fig. 4 Reflection and transmission upon a joint and the coordinate conventions Mitrou *et al.* (2017)

The FE joint is assumed to be infinite in the direction normal to the propagation one. This assumption, as we will see later, does not affect the results even for finite-size structures. It is to be underlined that there is no restriction on the type of FE model to be used for the joint. Even complex shapes can be modelled.

The main assumption which is made of the junction is that there are no forces applied on the inner points of its FE model. This easily allows the use of a condensation to the borders and express the dynamic equation of the junction as condensed to its edges (Eq. (18)). A typical method that can be used is the one showed in Eq. (7), or a component mode synthesis.

$$\mathbf{D}_j \mathbf{Q}_j = \mathbf{F}_j \quad (18)$$

Where \mathbf{Q}_j and \mathbf{F}_j are the vectors of dofs and nodal forces of the joint to its borders.

Since the force and displacement vectors at the borders of the joint are in common with the two waveguides, they can be expressed in wave base using the wavemodes of each periodic substructure. These must be expressed, however, in the same coordinate system. For this reason imposing the continuity and equilibrium conditions for the joint one has

$$\mathbf{Q}_j = \mathbf{R} \begin{Bmatrix} \mathbf{Q}_1 \\ \mathbf{Q}_2 \end{Bmatrix} \quad \mathbf{F}_j = \mathbf{R} \begin{Bmatrix} \mathbf{F}_1 \\ \mathbf{F}_2 \end{Bmatrix}$$

where

$$\mathbf{R} = \begin{bmatrix} \mathbf{R}_1 & \mathbf{0} \\ \mathbf{0} & \mathbf{R}_2 \end{bmatrix}$$

is a block diagonal matrix that includes the rotational matrices of the first and second waveguide. The approach followed is similar to the one proposed in [17]. In this case it is necessary to underline that

the coordinate system, as identified in Fig. 4, in not left-handed and thus attention has to be posed to the coordinate z .

Then the eigenvectors of the two waveguides can be used to express the displacements $\mathbf{Q}_{1,2}$ and the force field $\mathbf{F}_{1,2}$ in wave base.

$$\mathbf{Q}_j = \mathbf{R} \left\{ \Phi_q^{in} \begin{Bmatrix} \mathbf{a}_1^+ \\ \mathbf{a}_2^+ \end{Bmatrix} + \Phi_q^{out} \begin{Bmatrix} \mathbf{a}_1^- \\ \mathbf{a}_2^- \end{Bmatrix} \right\}$$

$$\mathbf{F}_j = \mathbf{R} \left\{ \Phi_f^{in} \begin{Bmatrix} \mathbf{a}_1^+ \\ \mathbf{a}_2^+ \end{Bmatrix} + \Phi_f^{out} \begin{Bmatrix} \mathbf{a}_1^- \\ \mathbf{a}_2^- \end{Bmatrix} \right\}$$

where, according to Fig. 4, the wavemodes matrices are expressed as follows

$$\Phi_q^{in} = \begin{bmatrix} \Phi_q^{1,+} & \mathbf{0} \\ \mathbf{0} & \Phi_q^{2,+} \end{bmatrix}$$

and

$$\Phi_q^{out} = \begin{bmatrix} \Phi_q^{1,-} & \mathbf{0} \\ \mathbf{0} & \Phi_q^{2,-} \end{bmatrix}$$

Substituting the previous equations in the equilibrium equation of the joint (Eq. 18), condensed to boundaries, one obtains the following expression

$$[\mathbf{D}_j \mathbf{R} \Phi_q^{in} - \mathbf{R} \Phi_f^{in}] \begin{Bmatrix} \mathbf{a}_1^+ \\ \mathbf{a}_2^+ \end{Bmatrix} = [\mathbf{R} \Phi_f^{out} - \mathbf{D}_j \mathbf{R} \Phi_q^{out}] \begin{Bmatrix} \mathbf{a}_1^- \\ \mathbf{a}_2^- \end{Bmatrix}$$

This way the scattering matrix can be obtained straightforwardly.

$$\mathbf{s} = - [-\mathbf{R} \Phi_f^{out} + \mathbf{D}_j \mathbf{R} \Phi_q^{out}]^{-1} [\mathbf{D}_j \mathbf{R} \Phi_q^{in} - \mathbf{R} \Phi_f^{in}]$$

The inversion in the previous equation can cause numerical instabilities and the use of the left eigenvalues is required Mitrou *et al.* (2017), as in the case of section 3.1.

Once the scattering matrix is calculated it is of fundamental importance for clearness in next steps to rewrite it in the following way.

$$\mathbf{s} = \begin{bmatrix} \mathbf{s}_1 & \mathbf{s}_2 \\ \mathbf{s}_3 & \mathbf{s}_4 \end{bmatrix}$$

It should be underlined that the actual description is applicable also for lap joints, L-shaped, T-shaped or more complex junctions, as deeply investigated in Renno *et al.* (2013) and Mitrou *et al.* (2017).

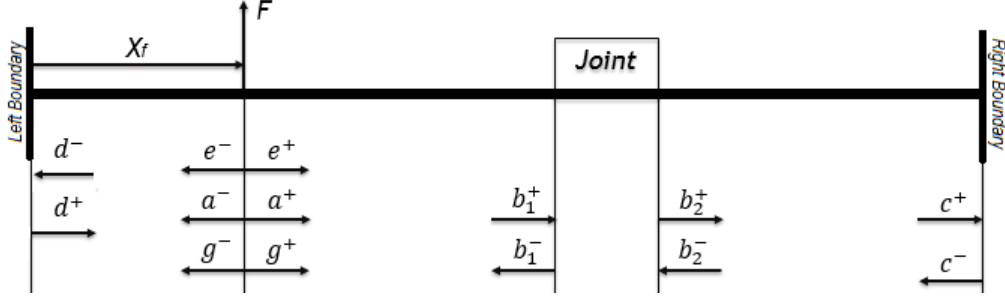


Fig. 5 Waves in a finite structure with a joint excited by a point load

4.2 Wave amplitudes in presence of scattering

The simple sketch in Fig. 5 shows the equilibrium equations for the wave amplitudes in the hybrid system. The equation of equilibrium are the same as in the standard case with the exception of the presence of the scattering at the joint.

The following is the set of equilibrium equation. Again it is remarked that the whole set is made of algebraic equations in matrix form.

At the excitation location, one can sum the incident and direct field, thus

$$\begin{aligned} a^+ &= e^+ + g^+ \\ g^- &= e^- + a^- \end{aligned} \quad (19)$$

At the very boundaries the following reflection relations are valid

$$\begin{aligned} c^- &= \mathbf{R}_{right}c^+ \\ d^+ &= \mathbf{R}_{left}d^- \end{aligned} \quad (20)$$

At the same time along the waveguide, the following propagation relations hold

$$\begin{aligned} g^+ &= \mathbf{Tr}(x_f)d^+ \\ d^- &= \mathbf{Tr}(x_f)g^- \\ a^- &= \mathbf{Tr}(L_1 - x_f)b_1^- \\ b_1^+ &= \mathbf{Tr}(L_1 - x_f)a^+ \\ c^+ &= \mathbf{Tr}(L_2)b_2^+ \\ b_2^- &= \mathbf{Tr}(L_2)c^- \end{aligned} \quad (21)$$

With L_1 and L_2 the lengths of the first (left) and second (right) waveguide. Moreover we need to include the scattering at the joint boundaries

$$\begin{Bmatrix} \mathbf{b}_1^- \\ \mathbf{b}_2^+ \end{Bmatrix} = \begin{bmatrix} \mathbf{s}_1 & \mathbf{s}_2 \\ \mathbf{s}_3 & \mathbf{s}_4 \end{bmatrix} \begin{Bmatrix} \mathbf{b}_1^+ \\ \mathbf{b}_2^- \end{Bmatrix}$$

Now, using all the previous equations the wave amplitudes can be evaluated in the driving point, in this case, the excitation location. Before doing that the scattering equation can be solved obtaining the values of the incoming and out-coming waves at the joint.

$$b_2^+ = [\mathbf{I} - \mathbf{s}_4 \mathbf{Tr}(L_2) \mathbf{R}_{left} \mathbf{Tr}(L_2)]^{-1} [\mathbf{s}_3 \mathbf{Tr}(L_1 - x_f)] a^+ \quad (22)$$

substituting in the other equation which derives from the scattering one we get

$$b_1^- = \mathbf{s}_1 \mathbf{Tr}(L_1 - x_f) a^+ + \mathbf{s}_2 \mathbf{Tr}(L_2) \mathbf{R}_{left} \mathbf{Tr}(L_2) b_2^+ \quad (23)$$

Substituting everything in Eq. (19), the following form of the wave amplitudes is derived, assuming, in this case, that the force is applied on the first waveguide.

$$\begin{aligned} a^+ = & [\mathbf{I} - \mathbf{Tr}(x_f) \mathbf{R}_{left} \mathbf{Tr}(x_f) \mathbf{Tr}(L_1 - x_f) \mathbf{s}_2 \mathbf{Tr}(L_2) \mathbf{R}_{left} \mathbf{Tr}(L_2) [\mathbf{I} - \mathbf{s}_4 \mathbf{Tr}(L_2) \mathbf{R}_{left} \mathbf{Tr}(L_2)]^{-1} \\ & \mathbf{s}_3 \mathbf{Tr}(L_1 - x_f) - \mathbf{Tr}(x_f) \mathbf{R}_{left} \mathbf{Tr}(x_f) \mathbf{Tr}(L_1 - x_f) \mathbf{s}_1 \mathbf{Tr}(L_1 - x_f)]^{-1} \\ & [e^+ + \mathbf{Tr}(x_f) \mathbf{R}_{left} \mathbf{Tr}(x_f) e^-] \end{aligned} \quad (24)$$

$$\begin{aligned} a^- = & \mathbf{Tr}(L_1 - x_f) [\mathbf{s}_2 \mathbf{Tr}(L_2) \mathbf{R}_{left} \mathbf{Tr}(L_2) [\mathbf{I} - \mathbf{s}_4 \mathbf{Tr}(L_2) \mathbf{R}_{left} \mathbf{Tr}(L_2)]^{-1} \\ & \mathbf{s}_3 \mathbf{Tr}(L_1 - x_f) - \mathbf{s}_1 \mathbf{Tr}(L_1 - x_f)] a^+ \end{aligned} \quad (25)$$

The wave amplitudes in the reception point can be then calculated applying the propagation relations, as done in the case of the simple WFE formulation. Using the wave base the displacements at the response point are expressed as such.

5. Numerical results

5.1 Test case: In-plane jointed panel

With reference to Fig. 3, lets consider two isotropic panels, our waveguides, connected through a 2D in-plane junction, discretised using FE. Free-Free boundary conditions will be implemented.

The hybrid method proposed will be used to analyse the vibrations on the first (left) waveguide for a point force applied in the same domain. The FE model on the junction has been condensed using the method showed in Eq. (7).

As noticeable in Fig. 6 the accuracy of the present method is excellent in the whole frequency range of analysis.

Table 1 Cylinder and hat-stiffener geometry

<i>Length</i>	4.2 m	<i>Height</i>	$3.0 \cdot 10^{-2} \text{ m}$
<i>Diameter</i>	2.8 m	<i>Thickness</i>	$5.0 \cdot 10^{-3} \text{ m}$
<i>Skins Thickness</i>	$4.0 \cdot 10^{-3} \text{ m}$	<i>Upper Width</i>	$2.0 \cdot 10^{-2} \text{ m}$
<i>Frames Thickness</i>	$7.0 \cdot 10^{-3} \text{ m}$	<i>Lower Width</i>	$3.0 \cdot 10^{-2} \text{ m}$

5.2 Stiffened cylinder

In the following case a doubly stiffened cylinder, as in the case of a simple aircraft fuselage, has been investigated. Frames and stiffeners are used to recreate the fuselage. The skins are modelled using a composite material whose data are available in Table 1, while the frames and the stiffeners are in aluminium. The model is periodic and composed of 37 identical substructures.

In the following Tables 2 and 1, the geometry and the material used for the skin used are shown. This are modelled using *ANSYS SOLID₄₅* elements, as the frames, while the stringers are modelled using *BEAM₄₄* elements.

Table 2 Material constants for cylinder skins

E_x	E_y	G_{xy}	ν_{xy}	Layup
125 GPa	12.5 GPa	6.89 GPa	0.38	$[0, 90, +45, -45, 0]_{sym}$

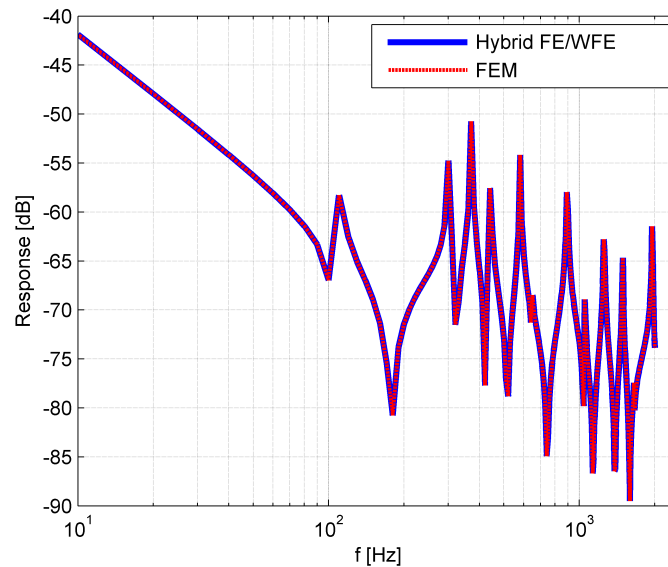


Fig. 6 FRF for forced displacements on the first waveguide. FEM full calculation (- red); Present Method (O-blue)

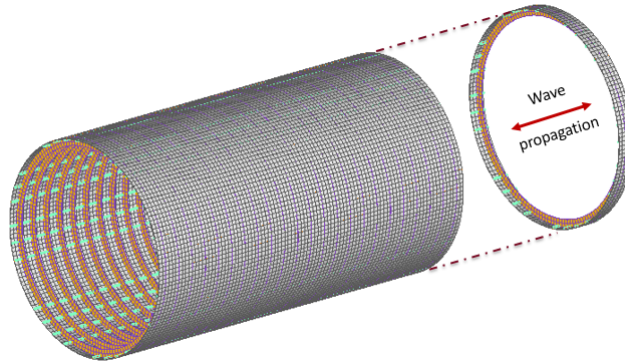


Fig. 7 Stiffened cylinder and the substructure used for the analysis of the wave propagation

In this case the filtering criteria is a $\text{imag}|k_i L_i| < 9.0$. As said the parameter has to be changed case-by-case and thus an optimal value has to be found to reduce the numerical issues.

The excitation is provided with four out-of-plane radial forces applied at $1/3$ of the cylinder length. The response is calculated at $1/2$ of the length instead. The wave-based model provides an overall accurate response (Fig. 8). However, especially if the damping and the filtering criteria are not properly set, the solution might detach from the FEM one. This is caused, again, by the inclusion, in response computing, of some wavemodes which are far from propagating at that frequency. This is not a conceptual mistake, since the principle is the same adopted in classic modal analysis when

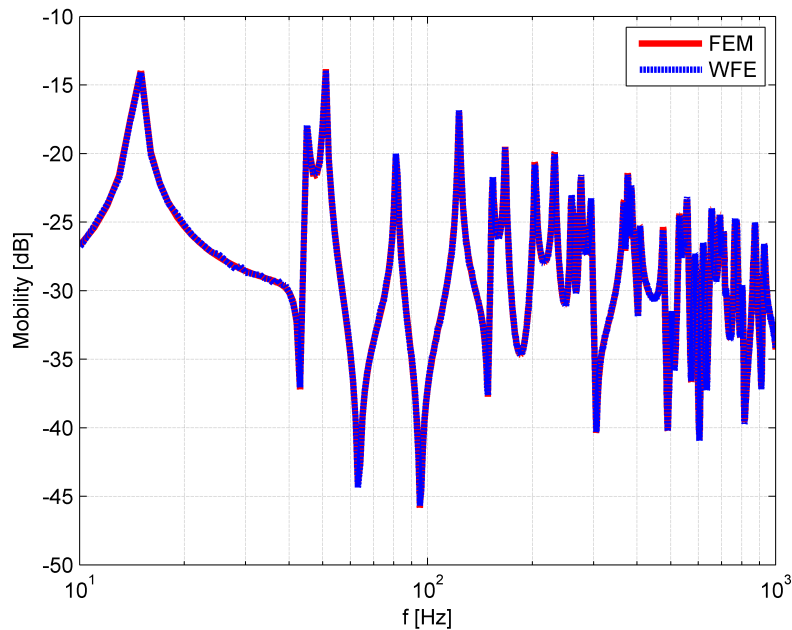


Fig. 8 FRF Mobility on the skin of the doubly stiffened cylinder. FEM full calculation (- red); WFE (- blue)

Table 3 Problem size in terms of DoF

<i>FEM</i> :	72680 DoF	
<i>WFEM</i> :	1920 DoF	Save = 97.36%

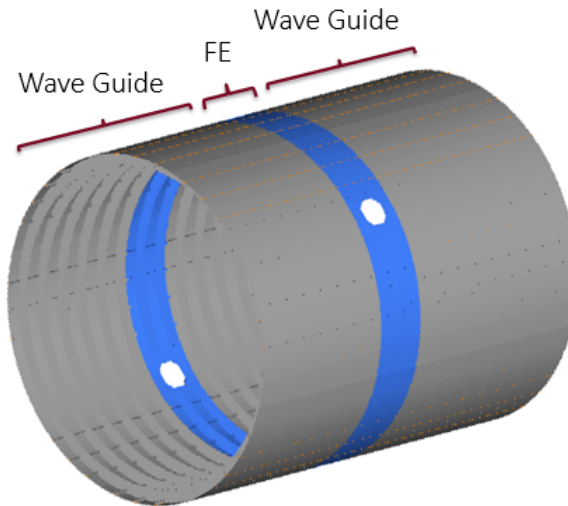


Fig. 9 Two waveguides (stiffened cylinders) connected with a complex junction

one can decide to consider all the structural modes outside the frequency band of interest, but causes numerical conditioning.

The saved computational cost is very high since the problem size is extremely reduced in terms of degrees of freedom, as shown in Table 3.

5.3 Stiffened cylinders with non-periodic holes

With reference to Fig. 9 the same cylinder model as before is considered as a waveguide but connected through a complex junction. The idea is to simulate, even if in a simplified model, the presence of windows in aircraft fuselages. This specific part, so, will be modelled using FE and condensed to the borders using a CB (Craig-Bampton) method, retaining 200 modes. The procedure used to analyse the response of the structure to a point load acting out-of-plane is the hybrid one proposed in section 4. The results in Fig. 10 show a good accuracy in the whole frequency range even if the numerical issues that arise in complex cases like this are exponentially higher than the one encountered in subsection 5.1, due to the inversion of the scattering matrix and the wavemodes filtering.

6. Conclusions

A basic and hybrid methodology involving the wave propagation in the periodic or semi-periodic media has been described. It allows a reduced computational cost when analysing the forced response of this category of structures.

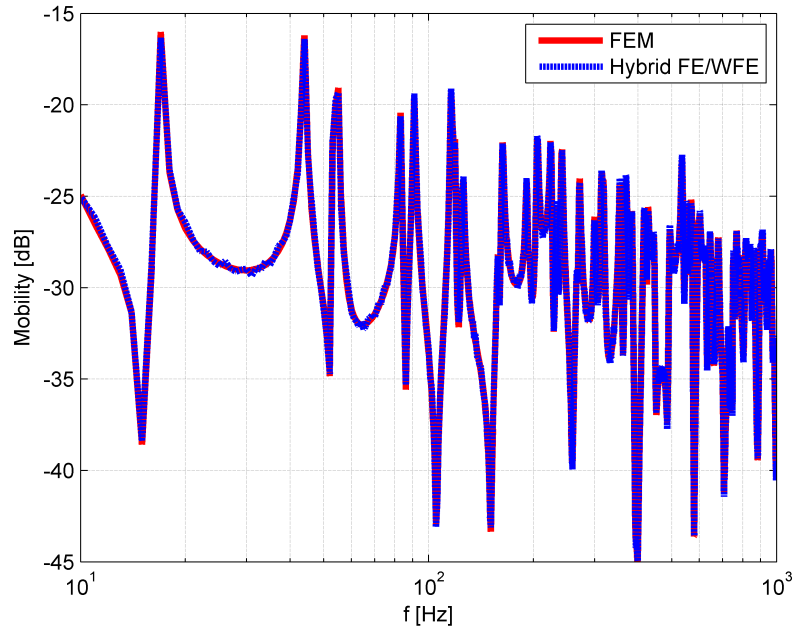


Fig. 10 FRF Mobility on the skin of the first waveguide of Fig. 9. FEM full calculation (- red); WFE (- blue)

The methodology, even if requiring an intense control in order to minimize the numerical conditioning, proved being very accurate in predicting the FRF for any position of the excitation and response. An extension to distributed loads is immediate.

The hybrid procedure and the scattering matrix description can be applied in any case, even for complex shapes and orientations of the waveguides and the junction. This makes the approach quite flexible to different industrial applications.

Acknowledgments

This project has received funding from the European Union's Horizon 2020 research and innovation program under the Marie Skłodowska-Curie grant agreement No. 675441. The author would like to gratefully acknowledge everyone involved in the VIPER project.

References

- Barbieri, E., De Rosa, S., Cammarano, A. and Franco, F. (2009), "Waveguides of a composite plate by using the spectral finite element approach", *J. Vib. Contr.*, **15**(3), 347–367.
- Brillouin, L. (1953), *Wave Propagation in Periodic Structures: Electric Filters and Crystal Lattices*, 2nd Edition, Dover Publications, INC., Mineola, New York, U.S.A.
- Chronopoulos, D., Troclet, B., Bareille, O. and Ichchou, M. (2013), "Modeling the response of composite panels by a dynamic stiffness approach", *Compos. Struct.*, **96**, 111-120.
- Chronopoulos, D., Troclet, B., Bareille, O. and Ichchou, M. (2014), "Computing the broadband vibroacoustic

- response of arbitrarily thick layered panels by a wave finite element approach”, *Appl. Acoust.*, **77**, 89–98.
- Cotoni, V., Langley, R.S. and Shorter, P.J. (2008), ”A statistical energy analysis subsystem formulation using finite element and periodic structure theory”, *J. Sound Vibr.*, **318**, 1077–1108.
- D’Alessandro, V. (2014), ”Investigation and assessment of the wave and finite element method for structural waveguides”, Ph.D. Dissertation, University of Naples Federico II, Italy.
- Manconi, E. and Mace, B.R. (2008), ”Modelling wave propagation in two dimensional structures using finite element analysis”, *J. Sound Vibr.*, **318**(4–5), 884–902.
- Mead, D.J. (1996), ”Wave propagation in continuous periodic structures: Research contributions from Southampton”, *J. Sound Vibr.*, **190**(3), 495–524.
- Mencik, J.M. and Ichchou, M.N. (2007), ”Wave finite elements in guided elastodynamics with internal fluid”, *J. Sol. Struct.*, **44**(7-8), 2148–2167.
- Mencik, J.M. (2010), ”On the low- and mid-frequency forced response of elastic structures using wave finite elements with one-dimensional propagation”, *Comput. Struct.*, **88** 674–689.
- Mitrou, G., Ferguson, N. and Renno, J. (2017), ”Wave transmission through two-dimensional structures by the hybrid FE/WFE approach”, *J. Sound Vibr.*, **389**, 484–501.
- Renno, J.M. and Mace, B.R. (2014), ”Calculating the forced response of cylinders using the wave and finite element method”, *J. Sound Vibr.*, **333**, 5340–5355.
- Renno, J. and Mace, B. (2013), ”Calculation of the reflection and transmission coefficients of joints using a hybrid finite element/wave finite element approach”, *J. Sound Vibr.*, **332**, 2149–2164.
- Waki, Y., Mace, B.R. and Brennan, M.J. (2009), ”Numerical issues concerning the wave and finite element method for free and forced vibrations of waveguides”, *J. Sound Vibr.*, **327**, 92–108.

EC